Quantum Electronics **49** (4) 386–390 (2019)

https://doi.org/10.1070/QEL16941

Electron parametric instabilities in nonuniform plasma with a strong density gradient excited by femtosecond laser pulses of subrelativistic intensity

I.N. Tsymbalov, D.A. Gorlova, V.Yu. Bychenkov, A.B. Savel'ev

Abstract. **We consider the excitation of electron parametric instability in the oblique incidence of femtosecond laser radiation of subrelativistic intensity on a plasma with the nonuniformity scale length of the order of the radiation wavelength λ. Estimates are obtained for two-plasmon decay instability increments in this plasma, and the generation of plasma waves due to parametric instabilities is numerically simulated by the particle-in-cell technique. The spatial spectrum of these waves is shown to broaden to the level corresponding to several values of the wavenumber k_0 of the component aligned with the electron density gradient and the wavenumbers of the component normal to the gradient have values $\sim k_0$.**

Keywords: *femtosecond laser plasma, parametric instabilities, two-plasmon decay, strong density gradient.*

1. Introduction

The plasma produced by an ultrashort pulse of relativistic intensity is a bright source of electrons accelerated to a high energy [1–3]. This source may find a variety of applications in the fields like laboratory astrophysics [4], investigations of nuclear reactions [5], electron and X-ray microscopy [6], etc. Trapping and acceleration of electrons may occur in the plasma wave breaking due to the quasi-static electric fields remaining after the breaking [7]. In a real experiment, plasma is produced by a prepulse prior to the arrival of the main ultrashort pulse, and plasma waves are therefore produced by the ultrashort pulse in the plasma density gradient. In this case, one of the main reasons for the excitation of plasma waves is the parametric instability in the vicinity of the quarter critical density $n_{e/4}$.

Parametric processes have been studied in detail in the case of the interaction of nanosecond laser pulses with a quasi-uniform plasma (i.e. the plasma in which the density gradient scale length $L = n_e(\mathrm{d}n_e/\mathrm{d}x)^{-1}$ is much longer than the laser wavelength λ) [8, 9]. We emphasise that the condition $L \gg \lambda$ is almost always fulfilled for nanosecond pulses. In the case of ultrashort pulses this condition is violated, and the situation in which $L \leqslant \lambda$ is quite typical, i.e. the plasma wave is localised in a very thin layer. Furthermore, the short duration of a femtosecond laser pulse requires investigating the issue of whether the instability growth rate is sufficiently high to excite the plasma wave of significant amplitude during the action of this pulse.

This situation has been poorly studied. Specifically, Veisz et. al. [10, 11] investigated the parametric instabilities in the case of interaction of a femtosecond laser pulse with a long density gradient and these results cannot be extended directly to the case of short plasma gradients. As far as we know, the only work on the experimental investigation carried out with short plasma gradients and femtosecond laser pulses was that by Tarasevitch et al. [12]. They interpreted the observed effects (the angular dependences of plasma radiation at the frequency equal to 3/2 of the heating radiation frequency ω_0) in the plane wave approximation, which is inapplicable in the case of short density gradients.

The aim of our work is to numerically investigate the excitation of plasma waves when a high-intensity femtosecond laser pulse is obliquely incident on the plasma with $L \sim \lambda$. The simulations are carried out by taking into account the broad angular spectrum of the pump wave due to a tight radiation focusing onto the target as well as to a gradual turn of the beam owing to its refraction in the gradient region.

In Ref. [13] we outlined the results of an experiment on plasma wave excitation and electron acceleration in the plasma with a short gradient scale length, which were combined with numerical simulations for the initial conditions corresponding to the experimental ones. In this work we also present estimates for the case of gradient scale length $L \sim \lambda$, which we take as the initial ones. To study in detail the excitation of plasma waves, we performed simulations for a lower intensity and a longer laser pulse duration than those in Ref. [13]. This significantly simplified the observed picture and allowed us to develop methods for analysing the temporal and spatial plasma density distributions obtained in our simulations.

Our simulations were performed with 3D3V pic-code MANDOR in 2D3V mode [14]. The plasma profile was specified as $n_e = n_0 \exp(y/L)$, where y is the coordinate along the inward-directed normal to the target measured from the initial target surface. Parameter n_0 was selected in such a way that the density varied from $0.01n_c$ to $4n_c$ in that part of the simulation domain where the plasma was produced. The size of the simulation box was 36×14 μm, the temporal and spatial resolutions of the numerical grid were 0.003 fs and 0.01 μm, respectively. Temporal and spatial envelopes of the laser pulse were Gaussian with a peak intensity of 10^{17} W

I.N. Tsymbalov, D.A. Gorlova Faculty of Physics and International Laser Center, M.V. Lomonosov Moscow State University, Vorob'evy Gory, 119991 Moscow, Russia; e-mail: ivankrupenin2@gmail.com;
V.Yu. Bychenkov P.N. Lebedev Physical Institute, Russian Academy of Sciences, Leninsky prosp. 53, 119991 Moscow, Russia;
A.B. Savel'ev Faculty of Physics and International Laser Center, M.V. Lomonosov Moscow State University, Vorob'evy Gory, 119991 Moscow, Russia; P.N. Lebedev Physical Institute, Russian Academy of Sciences, Leninsky prosp. 53, 119991 Moscow, Russia

Received 23 November 2018; revision received 29 January 2019
Kvantovaya Elektronika **49** (4) 386–390 (2019)
Translated by E.N. Ragozin

cm^{-2}. The laser pulse had a duration of 100 fs FWHM and a diameter of 4 μm FWHM in the focal plane for a parameter $F/D \sim 10$ (F is the focal distance of the lens and D is the laser beam diameter). The interaction was investigated for angles of incidence ranging from 45° to 60°, the electric vector of the incident wave lying in the plane of incidence. The ions were immobile, and the initial electron temperature was equal to 100 eV. Stored in the simulations was the information about the fields in the plasma and its electron density with spatial and temporal steps that provided more than two points per cycle of the highest-frequency field harmonic of those present in the plasma. This enabled us to extract and analyse the plasma waves of interest using spatial and temporal Fourier filtration.

2. Instability analysis

We now turn to the analysis of plasma instabilities: two-plasmon decay instability and stimulated Raman scaterring. The two-plasmon decay instability is responsible for the generation of two plasma waves, with the beating of the pump wave (i.e. the laser electromagnetic wave) and the 1st plasma wave producing the ponderomotive force which results in the growth of the amplitude of the 2nd plasma wave, and vice versa [15, 16]. For a plane monochromatic pump wave in a uniform plasma, this instability has been well studied, and an analytical expression for its linear increment has been obtained [16]:

$$\gamma = \frac{|\boldsymbol{k}\boldsymbol{v}_{\mathrm{osc}}|}{4} \frac{|(\boldsymbol{k}-\boldsymbol{k}_0)^2 - k^2|}{k|\boldsymbol{k}-\boldsymbol{k}_0|}, \qquad (1)$$

where $\boldsymbol{k}$ and $\boldsymbol{k}_0$ are the wave vectors of one of the plasma waves and the pump wave and $\boldsymbol{v}_{\mathrm{osc}}$ is the oscillatory electron velocity in the pump wave. The highest increment is achieved on the hyperbola (see Fig. 1)

$$k_\perp^2 = k_\parallel(k_\parallel - k_0), \qquad (2)$$

where $k_\parallel$ and $k_\perp$ are the $\boldsymbol{k}$ components parallel and perpendicular to $\boldsymbol{k}_0$, respectively.

In the interaction with a nonuniform plasma with a rather short gradient scale length, the pump wave is not plane. Let us consider the propagation of a laser pulse in this plasma and select the coordinate system in such a way that the electron density is nonuniform only along the y coordinate (Fig. 2). The wave vector components of the incident radiation are then written as $k_x = k_0 \sin\alpha$ and $k_y = k_0 \cos\alpha$, where α is the angle of incidence. Since the plasma permittivity depends only on the y component in our case, the x wave vector component will remain constant [17], while the y component will vary from $k_0\cos\alpha$ for the incident radiation to $-k_0\cos\alpha$ for the reflected one. In the case of a short plasma gradient scale length ($L \sim \lambda$), these spatial harmonics will form a wave packet localised near the turning surface corresponding to $n_{\mathrm{e\,turn}} = n_{\mathrm{c}}\cos^2\alpha$. Therefore, the pump may be represented as a superposition of plane waves whose spatial spectrum is represented in Fig. 2b.

We note that the expression for the two-plasmon decay instability increment was given by Follett et al. [18] for a finite number of pump waves symmetric with respect to one of the plasmons. However, there is no way of generalising it to an arbitrary continuous set of pump waves. Nevertheless it is possible to make a crude estimate of the regions of possible amplification of plasma waves by dividing the spatial spectrum of the laser pulse into parts of relatively small width $\Delta\boldsymbol{k}_0$

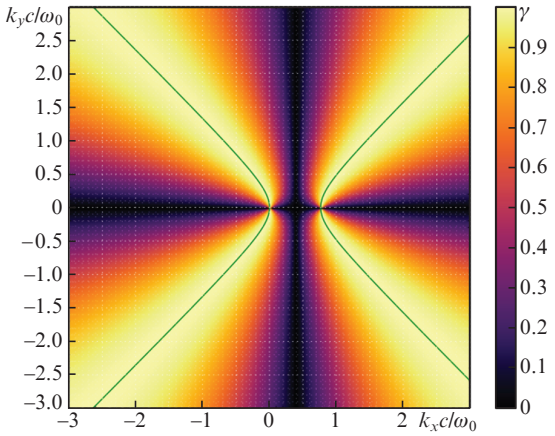

Figure 1. Normalised increment of the two-plasmon decay instability in a uniform cold plasma (ω_0 is the pump wave frequency).

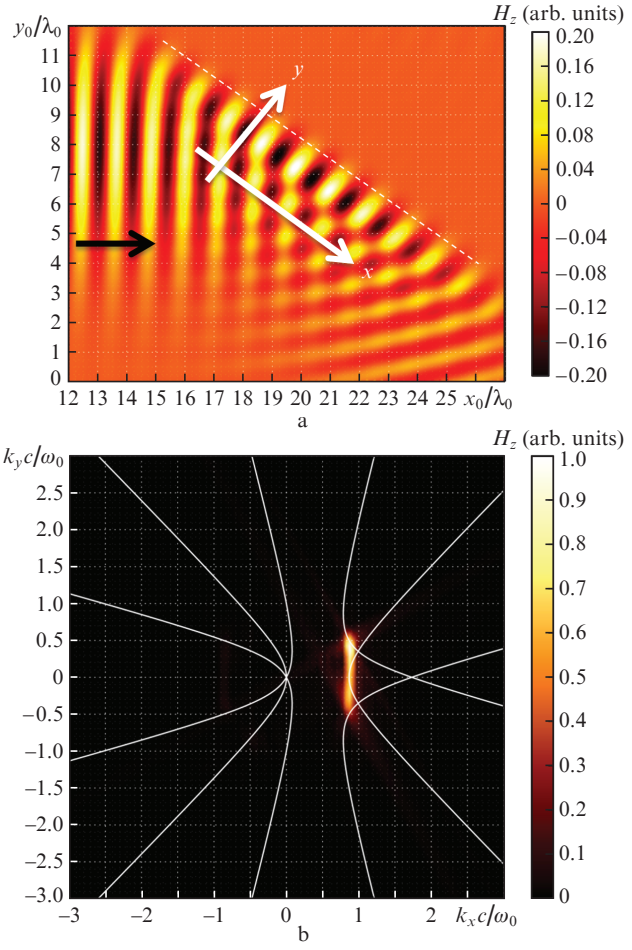

Figure 2. Reflection of a laser pulse for $L/\lambda = 1.25$ and an angle of incidence of 45°: (a) magnetic field magnitude H_z (in units of dimensionless vector potential) in relation to coordinates and (b) spatial field spectrum normalised to its peak value. The data were obtained by PIC simulations. The solid curves are the maximum growth rate hyperbolas (2) calculated for the incident, directed along the surface and reflected pump waves. The dashed line corresponds to the critical density n_{c}.

so as to treat the corresponding waves as plane ones and sum increments (1) for each wave vector $\boldsymbol{k}$ of the plasma wave:

$$\Gamma(\boldsymbol{k}) = \sum\nolimits_{\Delta k_0} \gamma(\boldsymbol{k}, \boldsymbol{k}_0, \boldsymbol{v}_{\mathrm{osc}}(\boldsymbol{k}_0)). \qquad (3)$$

The results of summation of the increments for different angles of incidence are given in Figs 3a, 3b, and 3c. Furthermore, also plotted are hyperbolas (2) corresponding to the peak increment for $k_y = k_0 \cos\alpha, 0$ and $-k_0 \cos\alpha$. As one can see, with decreasing angle of incidence from 60° to 45° there appear new amplification regions, which are uncharacteristic of the plane pump wave. This is confirmed by numerical simulations (Figs 3d, 3e, and 3f). At the same time, the spatial spectrum of the plasmons obtained by numerical simulations is significantly different from the spectra calculated by formula (3), i.e. amplification takes place not for arbitrary plasmon wave vectors.

The seed for plasma instability is provided by thermal noise; the initial temperature was equal to 100 eV. Early in the simulation, in the spatial plasma spectrum this allowed us to observe the components that were reasonably consistent with the peak increments calculated by formula (3) (Fig. 4). In this case, even after several cycles of the laser field the contribution of large-k components becomes smaller. At the same time, components with $k \sim 0$ are absent in Fig. 4 though they appear in Figs 3a–3c. This is due to the fact that our increment estimation only indicates possible regions of instability development, since phase relations are neglected in the summation. In the selected coordinate system, the pump has a narrow spatial spectrum in x and a broad one in y, and therefore it comes as no surprise that the spectrum of the plasma waves generated by the instabilities behaves in a similar way. We specify several plasma waves with indication of the x component of the wave vector. Amplified for $\alpha = 60°$ are two waves with $k_{1x} \approx 1.1\omega_0/c$ and $k_{2x} \approx -0.23\omega_0/c$ (Fig. 3c), with $k_{0x} \approx 0.87\omega_0/c$ for the pumping wave. Amplified for $\alpha = 45°$ are the waves with $k_{1x} \approx k_{2x} \approx 0.35\omega_0/c$ (Fig. 3a), with $k_{0x} \approx 0.71\omega_0/c$. When $\alpha = 50°$, an intermediate mode is observed with $k_{11x} \approx k_{21x} \approx 0.38\omega_0/c$ and $k_{12x} \approx 1.0\omega_0/c$, $k_{22x} \approx -0.13\omega_0/c$ (Fig. 3b), with $k_{0x} \approx 0.77\omega_0/c$. Therefore, the wavenumbers of several plasmons are near k_0, which is characteristic for stimulated Raman scattering (SRS) for $n_e \approx 0.25 n_c$ [19]. Consequently the observed disappearance of the components with a high spatial frequency and the enhancement of small-k waves could be explained as follows: apart from the two-plasmon decay instability, which results from the mutual amplification of the plasma waves by the beatings of their fields with the pumping wave field, the effect of SRS comes into play, which arises from the interaction of the Stokes wave with the pumping wave. The combined action of these two instabilities will be considered in greater detail in our next paper.

Figure 5a shows the plasma density perturbations obtained by simulations. One can see the parametric instability waves in the vicinity of the density $n_c/4$, the resonance excitation of plasma waves in the critical density domain, and the plasma oscillations along the surface caused by the linear transformation of the laser pulse at the turning point. Figure 5b shows only the waves near the $\omega_0/2$ frequency (we applied a

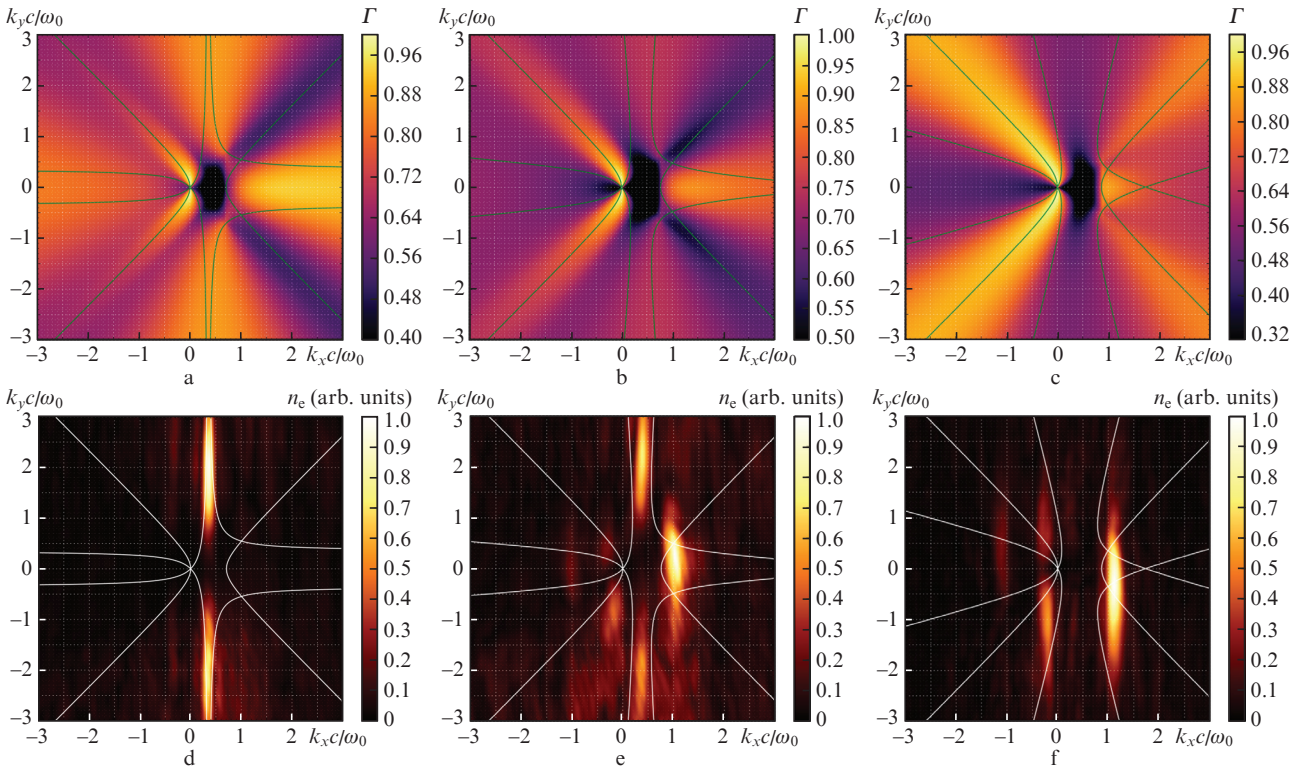

Figure 3. (a, b, c) Two-plasmon decay instability increment calculated by formula (3) for the pumping wave incident at different angles and (d, e, f) spatial spectra of the plasma density after bandpass filtering for selecting the $\omega_0/2$ frequency (filter bandpass from $\omega_0/4$ to $3\omega_0/4$), which were obtained by numerical simulations for $\alpha =$ (a, d) 45°, (b, e) 50°, and (c, f) 60°. The solid lines are hyperbolas (2). The magnitudes of the increments and the spectral amplitudes are normalised to their own peak values.

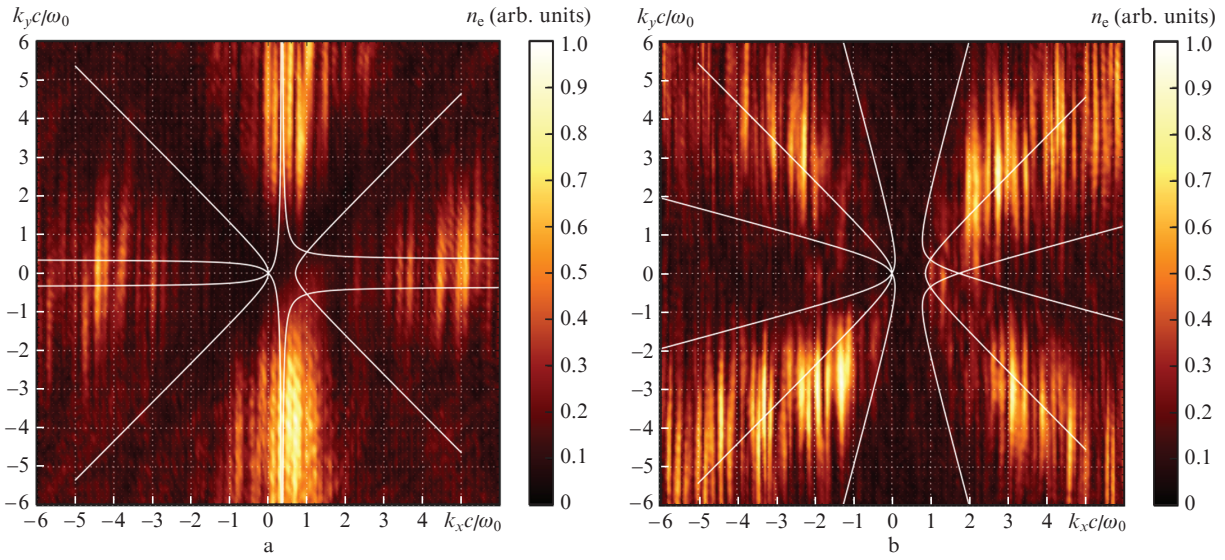

Figure 4. Spatial spectra of the plasma density after bandpass filtering for selecting the $\omega_0/2$ frequency at the initial stage of instability development. Presented are the simulation data for angles of incidence of (a) 45° and (b) 60°. The spectral amplitudes are normalised to their own peak values. The solid lines are the maximum growth-rate hyperbolas (2).

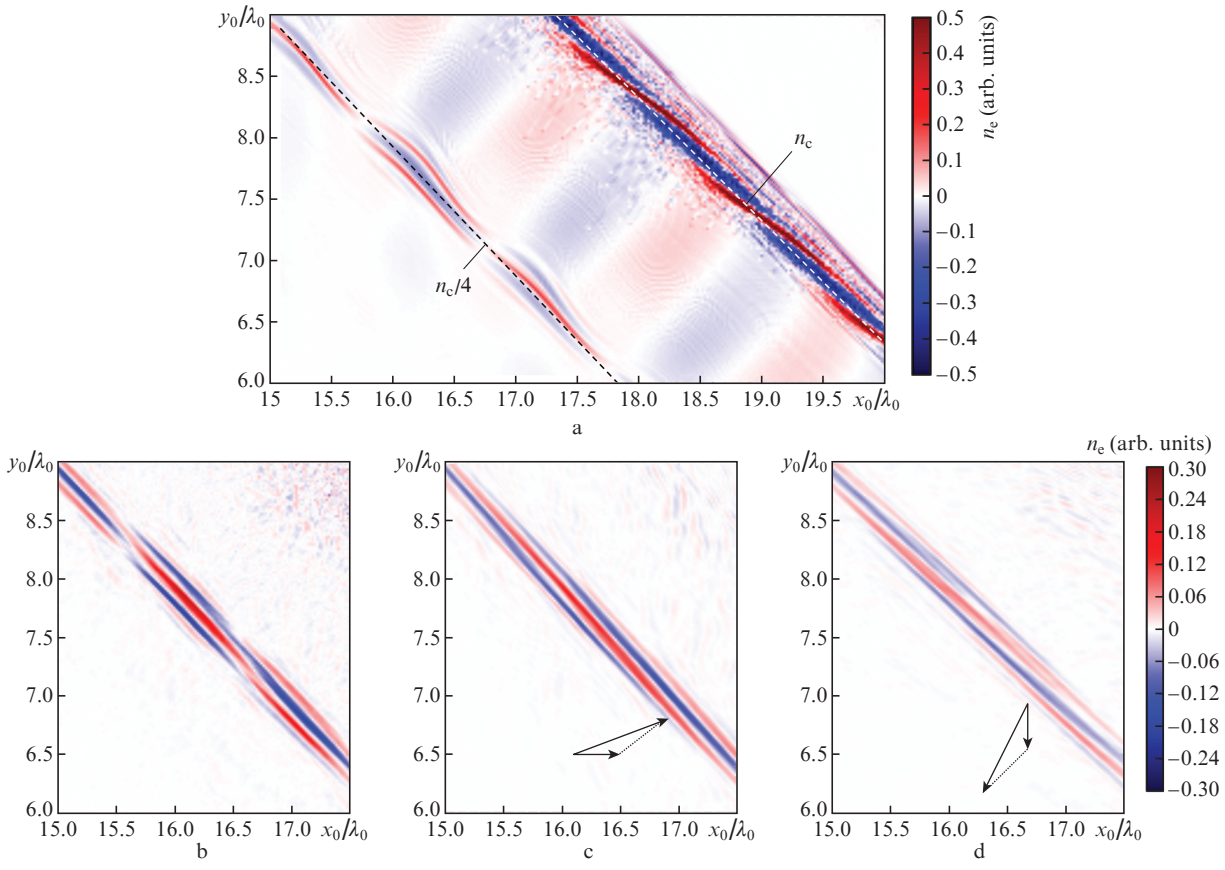

Figure 5. Fluctuations of the electron density relative to the initial one for an angle of incidence of 45° (a) as well as after bandpass filtering near the $\omega_0/2$ frequency (b) and the subsequent filtering in the spatial frequencies to select the waves $k_y > 0$ (c) and $k_y < 0$ (d). Shown schematically in Figs 5c and 5d are the variation ranges of the corresponding plasmon wave vectors. The fluctuation amplitudes n_e are normalised to the critical electron density n_c.

bandpass filter with a rectangular window from $\omega_0/4$ to $3\omega_0/4$). Two domains with $k_y > 0$ and $k_y < 0$, $k_x \approx 0.35\omega_0/c$, are present in the spatial spectrum (see Fig. 3d). Using the Fourier filter, we selected the waves with $k_y < 0$ (Fig. 5c) and $k_y > 0$ (Fig. 5d). One can see that the waves are localised in a narrow (of width $\sim\lambda$) region along the target surface near the

density $n_c/4$. Because of the low plasma temperature and the strong density gradient, these waves do not propagate beyond the region in which the ponderomotive forces exciting them are localised.

3. Conclusions

Therefore, the main feature of the electron plasma instabilities arising in the oblique incidence of laser radiation on a strongly nonuniform plasma ($L/\lambda \sim 1$) consists in that the excited waves possess a broad spatial spectrum $\Delta k \sim k$ along the axis aligned with the electron density gradient. This is because the spatial spectrum of the pump wave for these instabilities, i.e. of the laser pulse, undergoes similar changes during the reflection from the plasma density gradient. Early in the instability development, its spatial spectrum is well described by the expression for the two-plasmon decay instability increment calculated taking into account the spatial pumping spectrum. However, even for an intensity of 10^{17} W cm^{-2} after few laser-field cycles, there is a significant amplification of the spectral components with the wave vectors close to k_0. This is indication that stimulated Raman scattering comes into play in the amplification of plasma waves. The following values of the x projections of the wave vector of the plasma waves were obtained: $k_{1x} \approx 1.1\omega_0/c$ and $k_{2x} \approx -0.23\omega_0/c$ for $\alpha = 60°$ and $k_{1x} \approx k_{2x} \approx 0.35\omega_0/c$ for $\alpha = 45°$. We note the plasma waves may be diagnosed by measuring the characteristics of radiation at a frequency $3\omega_0/2$, which results from the scattering of the laser pulse on the generated plasmons.

Preliminary simulations suggest that this interaction picture holds for a plasma gradient scale length from 0.2λ to 5λ and intensities of up to 5×10^{19} W cm^{-2}. In this case, a modification of the plasma profile under light pressure and relativistic transparency comes into play. With increasing intensity, the plasma waves of parametric instabilities originate at stronger gradients: for an intensity of 5×10^{18} W cm^{-2} even for $L = 0.25\lambda$. However, at intensities above 5×10^{19} W cm^{-2} the plasma is too rapidly repulsed by ponderomotive forces for the instability to manage to develop. For a gradient scale length above 5λ, the SRS plasma waves are mainly observed.

Acknowledgements. This work was supported by the Russian Foundation for Basic Research (Grant Nos 18-32-00868 mol_a and 16-02-00263 A) and was carried out with the use of equipment of the Centre of Collective Use of Ultrahigh-Performance Computational Resources at Lomonosov Moscow State University.

References

1. Gibbon P., Förster E. *Plasma Physics and Controlled Fusion*, **38** (6), 769 (1996).
2. Mourou G.A., Tajima T., Bulanov S.V. *Rev. Modern Phys.*, **78**, 309 (2006).
3. Umstadter D. *J. Phys. D.*, **36**, 151 (2003).
4. Booth N. et al. *Nature Commun.*, **6**, 8742 (2015).
5. Tsymbalov I.N. et al. *Phys. Atomic Nuclei*, **80**, 397 (2017).
6. Najmudin Z. et al. *Phil. Trans. R. Soc. A.*, **372**, 20130032 (2014).
7. Esarey E., Schroeder C.B., Leemans W.P. *Rev. Modern Phys.*, **81**, 1229 (2009).
8. Afeyan B.B., Williams E.A. *Phys. Plasmas*, **4** (11), 3827 (1997).
9. Silin V.P. *Parametricheskoe vozdeistvie izlucheniya bol'shoi moshchnosti na plazmu* (Parametric Action of High-Power Radiation on a Plasma) (Moscow: Nauka, 1973).
10. Veisz L. et al. *Phys. Plasmas*, **9** (8), 3197 (2002).
11. Veisz L. et al. *Phys. Plasmas*, **11** (6), 3311 (2004).
12. Tarasevitch A. et al. *Phys. Rev. E.*, **68** (2), 026410 (2003).
13. Ivanov K.A. et al. *Phys. Plasmas*, **24** (6), 063109 (2017).
14. Romanov D.V., Bychenkov V.Yu., Rozmus W., Capjack C.E., Fedosejevs R. *Phys. Rev. Lett.*, **93**, 215004 (2004).
15. Mulser P., Bauer D. *High Power Laser-Matter Interaction* (Berlin: Springer, 2010) Vol. 238.
16. Kruer W. *The Physics of Laser Plasma Interactions* (Florida: CRC Press, 2018).
17. Ginzburg V.L. *The Propagation of Electromagnetic Waves in Plasmas* (Oxford: Pergamon Press, 1970; Moscow: Nauka, 1967).
18. Follett R.K. et al. *Phys. Plasmas*, **24** (10), 102134 (2017).
19. Quesnel B. et al. *Phys. Plasmas*, **4** (9), 3358 (1997).